Pro-Gastrin–Releasing Peptide as a Factor Predicting the Incidence of Brain Metastasis in Patients with Small Cell Lung Carcinoma with Limited Disease Receiving Prophylactic Cranial Irradiation

Kan Yonemori, M.D.
Minako Sumi, M.D.
Naoko Fujimoto, M.D.
Yoshinori Ito, M.D.
Atsushi Imai, M.D.
Yoshikazu Kagami, M.D.
Hiroshi Ikeda, M.D.

Division of Radiation Oncology, National Cancer Center Hospital, Tokyo, Japan.

BACKGROUND. Prophylactic cranial irradiation (PCI) reduces the incidence of brain metastasis with an effect on overall survival in patients with small cell lung carcinoma (SCLC). In spite of multidisciplinary intensive treatment approaches, many patients still experience brain metastasis. The authors retrospectively analyzed the characteristics of the first failure event due to brain metastasis (FBM) in patients treated with PCI.

METHODS. Between January 1990 and April 2004, 71 patients with limited disease SCLC were treated with PCI after completing systemic treatment at the National Cancer Center Hospital (Tokyo, Japan). Univariate and multivariate analyses were used to identify factors related to FBM and survival.

RESULTS. The FBM and overall incidence of brain metastasis (OBM) were 16.9 % (12 of 71) and 26.8% (19 of 71), respectively. Median time to progressive disease and median survival were 8.4 months and 21.6 months, respectively. Elevation of pro-gastrin–releasing peptide (Pro GRP) level before PCI was found to be a significant predictive and prognostic factor for FBM, OBM, and survival on multivariate analysis ($P = 0.007$, $P = 0.025$, and $P = 0.009$, respectively).

CONCLUSIONS. An elevated Pro GRP level before PCI was found to be significantly related to FBM and survival, and should be considered before PCI is performed. *Cancer* **2005;104:811–6.** © *2005 American Cancer Society.*

KEYWORDS: prophylactic cranial irradiation, small cell lung carcinoma, limited disease, predictive factor, pro-gastrin–releasing peptide.

Small cell lung carcinoma (SCLC) accounts for approximately 20% of all lung carcinomas.[1] Although SCLC rapidly develops distant metastasis, it is very sensitive to chemoradiotherapy, unlike non-SCLC. Limited disease SCLC is clinically confined to the hemithorax, and chemoradiotherapy is the standard treatment. In patients with limited disease SCLC, chemotherapy combined with thoracic radiotherapy yields complete remission (CR) rates of 50–85%, with a median survival time of 12–20 months.[2–4] The 5-year survival rate is reported to be 26% for patients who have CR.[4] Because chemoradiotherapy reduces the risk of intrathoracic disease recurrence, distant metastasis in the brain has been the main cause of disease recurrence. Although only 10% of patients have brain metastasis at the time of diagnosis, the cumulative incidence at 2 years is > 50%.[5,6] As many as 73% of patients develop clinically apparent central nervous system metastases before death,[7,8] and even higher rates are documented in autopsy series.[9] The brain is the initial site of disease recurrence in 5–

Address for reprints: Kan Yonemori, M.D., Division of Radiation Oncology, National Cancer Center Hospital, 5-1-1 Tsukiji, Chuo-ku, Tokyo, 104-0045, Japan; Fax: (011) 81-3-3542-3815; E-mail: kyonemor@ncc.go.jp

Received November 1, 2004; revision received March 7, 2005; accepted March 22, 2005.

DOI 10.1002/cncr.21238
Published online 22 June 2005 in Wiley InterScience (www.interscience.wiley.com).

33% of patients, and is the only site of disease recurrence in ≤ 20% of patients.[10,11]

Although several randomized trials of prophylactic cranial irradiation (PCI) have attempted to reduce the risk of brain metastasis and to improve survival, to our knowledge its role in the management of patients with SCLC has remained controversial according to the results of each trial.[12–14]

Recently, the metaanalysis of these trials comparing PCI with no-PCI found that PCI led to a small but significant absolute reduction in mortality (5.4%), and that PCI not only significantly reduced the risk of brain metastasis, but also improved both overall survival (OS) and disease-free survival among patients with SCLC in CR.[15] These results suggest that PCI should be considered as a part of the standard treatment for patients with limited disease SCLC who achieved CR or good partial remission (PR).

Although PCI was performed for patients who achieved CR or good PR as part of the combined treatment that consisted of chemotherapy and thoracic radiotherapy, brain metastasis occurred in 4–24% of the treated patients.[6,12–14] Whole-brain irradiation (WBRT) for brain recurrence was often difficult because these patients had already received PCI to the whole brain. Therefore, we should strictly consider PCI for patients who could achieve a true CR, as assessed with diagnostic imaging. In addition, we should be careful to follow the patients who have a high risk of brain recurrence after PCI.

To our knowledge, there are no previous reports that describe the characteristics of patients with brain metastasis after PCI. In the current study, we analyzed retrospectively predictive factors for brain metastasis in patients with limited disease SCLC treated with PCI.

MATERIALS AND METHODS

Patients

A total of 71 patients with limited disease SCLC were treated with PCI after chemoradiotherapy for primary disease between January 1990 and April 2004 at the National Cancer Center Hospital (Tokyo, Japan). Fifty-four patients were male, and the median age was 62 years old (range, 40–75 years).

Histologic or cytologic examination confirmed the diagnosis of SCLC in all patients. Before the initiation of systemic treatment, staging was performed using computed tomography (CT) or magnetic resonance imaging (MRI) scans of the chest, abdomen, and brain, as well as radionuclide bone scanning and bone marrow aspiration and biopsy. Limited disease was defined as being limited to one hemithorax, mediastinal, hilar, or supraclavicular area, which could be encompassed within a reasonable single radiation portal. Patients with pleural effusion found on chest films or CT scan were excluded.

Tumor response was classified in accordance with the World Health Organization (WHO) criteria.[16] After systemic treatment, including thoracic radiotherapy, PCI was administered to patients with CR or good PR according to the results of chest radiography and CT or MRI scans of the head, chest, and abdomen.

Thoracic Radiotherapy

The majority of patients (n = 55 [77.5%]) received accelerated twice-daily thoracic radiotherapy comprised of 45 gray (Gy) in 1.5-Gy fractions. The remaining patients (n = 16 [22.5%]) received once-daily radiotherapy, 50 Gy in 2-Gy fractions. Radiotherapy was performed 5 days per week, excluding weekends and holidays. Sixty of the 71 patients received concurrent chemoradiotherapy, which began on Day 2 of the first cycle of combination chemotherapy as cisplatin (80 mg/m^2, Day 1) plus etoposide (100 mg/m^2, Days 1, 2, and 3). The other patients received sequential thoracic radiotherapy after the forth cycle of chemotherapy.

The initial field included the primary tumor volume with a 1.5-cm margin around the mass, the ipsilateral hilum, the entire width of the mediastinum, and the supraclavicular lymph nodes (only if there was tumor involvement).

Chemotherapy

All patients received cisplatin combination chemotherapy. After concurrent chemoradiotherapy, 34 patients received 3 cycles of cisplatin plus etoposide, 17 patients received CODE therapy (cisplatin at a dose of 25 mg/m^2 weekly for 6 weeks; vincristine at a dose of 1 mg/m^2 during Weeks 2, 4, and 6; and doxorubicin at a dose of 40 mg/m^2 and etoposide at a dose of 80 mg/m^2 for 3 days during Weeks 1, 3, and 5), and 9 patients received 3 cycles of cisplatin (60 mg/m^2, Day 1) plus irinotecan (60 mg/m^2, Days 1, 8, 15). In patients treated with sequential radiotherapy, five patients received four cycles of cisplatin plus etoposide, four patients received four cycles of cisplatin plus irinotecan, and two patients received four cycles of cisplatin containing combination chemotherapy, optimized for each patient.

Prophylactic Cranial Irradiation

All patients who achieved CR (n =40 [56.3%]) or good PR (n = 31 [43.7%]) were treated with PCI. The median time between the initiation of systemic induction treatment and the initiation of PCI (duration) was 3.7 months (range, 2.6–7.5 months).

The target volume was the entire intracranial site. Individual shaped ports with multileaf collimators

were used to define the irradiation target volume. Patients were treated using a megavoltage linear accelerator with 4–6 megavolt (MV) photons. Treatment was delivered with equally weighted right and left lateral fields, with the dose calculated on the central ray at mid-separation of the beams.

Of the 71 patients who received PCI, the majority of patients (52 of 71 [73.2%]) received 25 Gy in 2.5-Gy fractions daily, 12 patients received 30 Gy in 2-Gy fractions daily, 6 patients received 24 Gy in 1.5-Gy fractions twice daily, and 1 patient received 36 Gy in 2-Gy fractions daily. All PCI was performed a total of 5 days per week. The treatment was administered with a linear accelerator of 6 MV (n = 53 patients) or 4 MV (n = 18 patients). The median follow-up time after PCI was 16.3 months (range, 1.4–113.6 months).

Statistical Analysis

The first failure event due to brain metastasis (FBM) was defined as brain metastasis as a first event after PCI, and the overall incidence of brain metastasis (OBM) was defined as the overall incidence of brain metastasis found throughout the clinical course after PCI. Clinical and laboratory variables before PCI were chosen by considering possible factors indicated by our own experience. We determined the predictive factors for FBM and OBM using both univariate (Pearson chi-square test/Fisher exact test) and multivariate analysis.

Before PCI, 9 categorized variables for multivariate analysis were selected, as follows: gender (male vs. female), age (< 60 vs. ≥ 60 years), response to systemic treatment (CR vs. good PR), time between the start of systemic treatment and the start of PCI (duration: < 4 months vs. ≥ 4 months), hemoglobin level (< 10 g/dL vs. ≥ 10 g/dL), lactate dehydrogenase level (≤ 229 U/L vs. > 229 U/L), C-reactive protein (≤ 0.1 mg/dL vs. > 0.1 mg/dL), neuron-specific enolase (NSE) (≤ 10 ng/mL vs. > 10 ng/mL), and pro-gastrin–releasing peptide (Pro GRP) (≤ 46 pg/mL vs. > 46 pg/mL).

Time to progressive disease (PD) was measured from the first day of PCI until PD or the last day of follow-up without PD, and OS time was measured from the first day of PCI until death or the last day of follow-up. Median time to PD and median OS were estimated using the Kaplan–Meier method. Prognostic factors were evaluated by multivariate analysis. All statistical analyses were performed using SPSS version 12.0J (SPSS Inc., Chicago, IL).

RESULTS

Incidence of Brain Metastasis

FBM and OBM were observed in 16.9% (12 of 71; 95% confidence interval [95% CI], 8.2–17.3%) and 26.8% (19 of 71; 95% CI, 16.5–27.3%) of patients, respectively. Nine patients with FBM had multiple brain metastases and the others had solitary lesions. Among these patients, six were reirradiated with WBRT or stereotactic multiarc radiotherapy, five were treated with systemic chemotherapy, and one received best supportive care. The median times to FBM and OBM were 9.4 months (range, 1.1–23.5 months) and 12.0 months (range, 1.1–92.9 months), respectively. In univariate analysis, an elevated Pro GRP level was found to be significantly related to FBM and OBM (Table 1) (P = 0.007 and P = 0.029, respectively). Using a complete dataset from

TABLE 1
Univariate Analyses of Pretreatment Variables for FBM and OBM

Variables	No. of patients	No. of FBM	P value	No. of OBM	P value
Gender			0.27		0.99
Male	54	11		15	
Female	17	1		4	
Age (yrs)			0.71		
≥ 60	38	7		11	0.66
< 60	33	5		8	
Energy (MV)			0.99		0.36
4	18	3		3	
6	53	9		16	
Total dose (Gy)			0.99		0.08
≤ 25	58	10		13	
> 25	13	2		6	
Hyperfraction			0.27		0.33
Twice daily	6	2		3	
Once daily	65	10		16	
Response			0.63		0.70
Good PR	31	6		9	
CR	40	6		10	
Duration (mos)[a]			0.61		0.86
≥ 4	25	5		7	
< 4	46	7		12	
Hemoglobin level (g/dL)			0.75		0.79
< 10	43	8		12	
≥ 10	28	4		7	
LDH level (U/L)			0.99		0.99
> 229	6	1		1	
≤ 229	65	11		18	
CRP level			0.75		0.50
> 0.1 mg/mL	42	8		10	
≤ 0.1 mg/dL	29	4		9	
NSE level (ng/mL)			0.63		0.99
> 10	8	2		2	
≤ 10	59	10		16	
Pro GRP level (pg/mL)			0.007		0.029
> 46	12	5		5	
≤ 46	37	2		4	

FBM: first failure event due to brain metastasis, OBM: overall incidence of brain metastasis, MV: megavolt; Gy: grays; PR: partial remission, CR: complete remission; LDH: lactate dehydrogenase, CRP: C-reactive protein; NSE: neuron- specific enolase; Pro GRP: pro-gastrin-releasing peptide.
[a] Duration indicates the time between the initiation of systemic induction treatment and the initiation of prophylactic cranial irradiation.

TABLE 2
First Progressive Disease Sites after PCI

Site	No. of patients	% of all patients
Local failure (inside the thorax)	20	28.2
Distant metastasis[a]	26	36.6
Abdominal organ	7	9.9
Bone	9	12.7
Spinal cord	1	1.4
Brain	12	16.9
Total	46	64.8

PCI: prophylactic cranial irradiation.
[a] Three patients had more than one progressive disease site in distant metastasis.

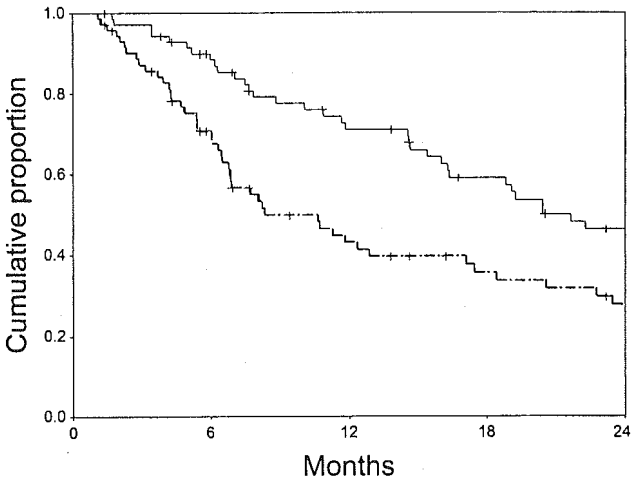

FIGURE 1. Kaplan–Meier analysis of time to disease progression (dotted line) and overall survival (solid line).

49 patients, a multivariate logistic regression model disclosed that an elevated Pro GRP level was a significant predictive factor for both FBM (hazard ratio [HR], 12.5; 95% CI, 2.00–77.9 [P = 0.007]) and OBM (HR, 5.89; 95% CI, 1.25–27.7 [P = 0.025]).

Time to Progressive Disease and Survival

In the current series, the majority of patients (46 of 71 [64.8%]; 95% CI, 53.7–65.4%) experienced PD in their clinical courses. The first sites of PD are listed in Table 2. The median time to PD and the median survival time were 8.4 months (95% CI, 3.9–12.8 months) (Fig. 1)and 21.6 months (95% CI, 14.1–29.2 months) (Fig. 1), respectively. A multivariate Cox regression model indicated that elevated Pro GRP level before PCI was a prognostic factor (HR, 2.97; 95% CI, 1.31–6.75 [P = 0.009]).

DISCUSSION

It is suggested that PCI eradicates subclinical brain metastasis that is protected from cytotoxic drugs by the blood-brain barrier as a pharmacologic sanctuary.[17] A recently reported metaanalysis of seven prospectively randomized trials demonstrated both an OS and disease-free survival advantage for patients with limited disease SCLC who received PCI compared with patients who did not receive PCI.[15] However, the metaanalysis included various trials and often insufficient systemic chemotherapy regimens, different PCI techniques, and a mixed population of patients with limited and extensive disease.[12–15] Therefore, Kotalik et al.[18] found there was insufficient evidence to make a definitive recommendation in terms of the total dose, fractionation, indication, and timing of PCI according to this metaanalysis.

In the current study, 16.9% of patients had brain metastasis as a first site of failure, which is consistent with previous reports of 4–24%.[6,12–14] The salvage treatment for brain metastasis after PCI would be restricted by the number of brain metastases, patient condition, and previous irradiation. To our knowledge, no report has described the predictive or prognostic factors for outcomes after PCI. Therefore, our results could provide useful information concerning the indication of PCI and close follow-up in patients with limited disease SCLC with CR or good PR who received intensive multidisciplinary treatment.

We found that elevated Pro GRP level before PCI was a significant predictive factor for FBM and for OBM (P = 0.007 and P = 0.025, respectively). The other pretreatment variables such as clinical and laboratory parameters had no influence on FBM or OBM. Among tumor markers, NSE is known to have a high false-positive rate due to hemolysis, whereas Pro GRP is a stable and reliable tumor marker for SCLC.[19] In addition Pro GRP is found to have higher specificity than NSE, and its serum level was frequently elevated at an earlier stage compared with that of the NSE level in patients with SCLC at the time of diagnosis.[20,21] It is reported that Pro GRP reflects tumor volume and the effect of treatment more sensitively than does NSE, and that it is useful in detecting PD because Pro GRP levels increase before disease recurrence becomes evident.[19,21,22] From the results of the current study, the elevation of Pro GRP before PCI might reflect the existence of residual viable tumor cells after a series of induction treatments, even if CR or good PR is indicated by imaging. A PCI would be recommended for patients with limited and extensive disease SCLC with CR.[15] However, PCI might not be sufficiently beneficial for decreasing the incidence of brain metastasis in patients with an elevated Pro GRP level. Therefore, by the completion of whole therapy, we should completely eliminate residual subclinical intracranial

and/or extracranial disease that causes the brain recurrence.

Several evidence-based guidelines for limited disease SCLC described uncertainty in terms of the optimal regimen, schedule of drug administration, duration of chemotherapy, and maintenance chemotherapy.[23,24] Although there is a guideline that recommends a maximum of six cycles of chemotherapy,[23] the trend in clinical trials and practice, including the current study, has been to use only four cycles of cisplatin-based chemotherapy. In patients with CR with elevated Pro GRP after four cycles of chemotherapy, two additional cycles of chemotherapy might be possible to eliminate tumor cells, to normalize Pro GRP levels, and to reduce the risk of brain recurrence.

A previous study suggested that there may be a dose-response relation for PCI, and that higher doses were more effective in reducing the risk of brain metastasis.[14] If currently ongoing trials that compare 25 Gy in 10 fractions with 36 Gy in 18 fractions[18] indicate the superiority of high-dose PCI, this will be another option to optimize the PCI procedure for controlling the subclinical disease at pharmacologic sanctuary.

The previous WHO criteria for evaluation of tumor response[11] did not consider the value of tumor markers. However, the Response Evaluation Criteria in Solid Tumors (RECIST) include tumor markers for assessment of CR.[25] Serum laboratory methods more accurately evaluate the evidence of viable tumor cells, and have a complementary role to the imaging studies when macroscopic tumor disappears or residual scar remains. In SCLC, tumor markers are well correlated to the response and tumor volume,[19,21,22] as was observed with Pro GRP in the current study. Therefore, CR according to the RECIST guidelines might be more appropriate in the evaluation of patients with SCLC for PCI.

Several authors reported many prognostic factors of clinical and laboratory parameters for patients with SCLC.[26] Almost all the analyses in the previous reports showed pretreatment factors before the initiation of systemic therapies. We analyzed pretreatment parameters for patients with CR or good PR receiving PCI. In our study, most of the laboratory parameters fell within normal limits before PCI, except for Pro GRP as a prognostic factor.

Local failure occurred in approximately one-half of the patients with disease recurrence, in addition to distant failure. The Southwest Oncology Group reported the pattern of failure in 114 patients with limited disease SCLC treated with cisplatin plus etoposide and concomitant thoracic radiotherapy followed by PCI. Local failure and distant metastasis occurred in 49% and 35% of patients, respectively.[27] These results also suggested that the main cause for disease recurrence was local or distant failure. Therefore, it is crucial to develop new drugs or regimens for improving local and distant control, which achieve a high rate of CR without elevation of tumor markers such as Pro GRP before PCI.

The results of the current study demonstrate that elevation of Pro GRP before PCI is a significant predictive factor for the first failure event due to brain metastasis. With regard to the indication of PCI, the assessment of clinical response according to RECIST might be evaluated more accurately using Pro GRP together with conventional imaging studies.

REFERENCES

1. Morita T, Sugano H. A statistical analysis of lung cancer registered in the annual of pathological autopsy cases in Japan between 1958 and 1987, with special reference to the characteristics of lung cancer in Japan. *Acta Pathol Jpn.* 1990;40:665–675.
2. Albain KS, Crowley JJ, LeBlanc M, Livingston RB. Determinants of improved outcome in small-cell lung cancer: an analysis of the 2,580 patient Southwest Oncology Group data base. *J Clin Oncol.* 1990;8:1563–1574.
3. Arriagada R, Kramar A, Le Chevalier T, De Cremoux H. Competing events determining relapse-free survival in limited small-cell lung carcinoma. *J Clin Oncol.* 1992;10:447–451.
4. Turrisi AT 3rd, Kim K, Blum R, et al. Twice-daily compared with once daily thoracic radiotherapy in limited small-cell lung cancer treated concurrently with cisplatin and etoposide. *N Engl J Med.* 1999;340:265–271.
5. Komaki R, Cox JD, Whitson W. Risk of brain metastasis from small cell carcinoma of the lung related to length of survival and prophylactic irradiation. *Cancer Treat Rep.* 1981;65:811–814.
6. Arriagada R, Le Chevalier T, Borie F, et al. Prophylactic cranial irradiation for patients with small-cell lung cancer in complete remission. *J Natl Cancer Inst.* 1995;87:183–190.
7. Hirsh FR, Paulson OB, Hansen HH, Larsen SO. Intracranial metastases in small cell carcinoma of the lung. Prognostic aspects. *Cancer.* 1983;51:529–533.
8. Eagan RT, Frytak S, Lee RE, Creagan ET, Ingle JN, Nichols WC. A case for preplanned thoracic and prophylactic whole brain radiation therapy in limited small cell lung cancer. *Cancer Clin Trials.* 1981;4:261–266.
9. Newman SJ, Hansen HH. Frequency, diagnosis, and treatment of brain metastases in 249 consecutive patients with bronchogenic carcinoma. *Cancer.* 1974;33:492–496.
10. Borgelt BB, Gelber R, Kramer S, et al. The palliation of brain metastases: final results of the first two studies by the Radiation Therapy Oncology Group. *Int J Radiat Oncol Biol Phys.* 1980;6:1–9.
11. Rosen ST, Makuch RW, Lichter AS, et al. Role of prophylactic cranial irradiation in prevention of central nervous system metastases in small cell lung cancer: potential benefit restricted to patients with complete response. *Am J Med.* 1983;74:615–624.

12. Maurer LH, Tulloh M, Weiss RB, et al. A randomized combined modality trial in small cell carcinoma of the lung: comparison of combination chemotherapy-radiation therapy versus cyclophosphamide-radiation therapy effects of maintenance chemotherapy and prophylactic whole brain irradiation. *Cancer.* 1980;45:30–39.
13. Hansen HH, Dombernowsky P, Hirsh FR, Hansen M, Rygard J. Prophylactic irradiation in bronchogenic small cell anaplastic carcinoma. A comparative trial of localized versus extensive radiotherapy including prophylactic brain irradiation in patients receiving combination chemotherapy. *Cancer.* 1980;46:279–284.
14. Gregor A, Cull A, Stephens RJ, et al. Prophylactic cranial irradiation is indicated following complete response to induction therapy in small cell lung cancer: results of multicentre randomized trial. United Kingdom Coordination Committee for Cancer Research (UKCCCR) and the European Organization for Research and Treatment of Cancer (EORTC). *Eur J Cancer.* 1997;33:1752–1758.
15. Auperin A, Arriagada R, Pignon JP, et al. Prophylactic cranial irradiation for patients with small-cell lung cancer in complete remission. Prophylactic Cranial Irradiation Overview Collaborative Group. *N Engl J Med.* 1999;341:475–484.
16. Miller AB, Hoogstraten B, Staquet M. Reporting results of cancer treatment. *Cancer.* 1981;147:207–214.
17. Hansen HH. Should initial treatment of small cell carcinoma include systemic chemotherapy and brain irradiation? *Cancer Chemother Rep.* 1973;4:239–241.
18. Kotalik J, Yu E, Markman BR, Evans WK. Cancer Care Ontario Practice Guidelines Initiative Lung Cancer Disease Site Group. Practice guideline on prophylactic cranial irradiation in small-cell lung cancer. *Int J Radiat Oncol Biol Phys.* 2001; 50:309–316.
19. Yamaguchi K, Aoyagi K, Urakami K, et al. Enzyme-linked immunosorbent assay of pro-gastrin-releasing peptide for small cell lung cancer patients in comparison with neuron-specific enolase measurement. *Jpn J Cancer Res.* 1995;86: 698–705.
20. Takada M, Kusunoki Y, Masuda N, et al. Pro-gastrin-releasing peptide (31-98) as a tumor marker of small-cell lung cancer: comparative evaluation with neuron-specific enolase. *Br J Cancer.* 1996;73:1227–1232.
21. Okusaka T, Eguchi K, Kasai T, et al. Serum levels of progastrin-releasing peptide for follow-up of patients with small-cell lung cancer. *Clin Cancer Res.* 1997;3:123–127.
22. Sunaga N, Tsuchiya S, Minato K, et al. Serum pro-gastrin-releasing peptide is a useful marker for treatment monitoring and survival in small-cell lung cancer. *Oncology.* 1999; 57:143–148.
23. Laurie SA, Logan D, Markman BR, Mackay, JA, Evans WK. Practice guideline for the role of combination chemotherapy in the initial management of limited-stage small-cell lung cancer. *Lung Cancer.* 2004;43:223–240.
24. Simon GR, Wagner H. Small cell lung cancer. *Chest.* 2003; 123:259S–271S.
25. Therasse P, Arbuck AG, Eisenhauer EA, et al. New guidelines to evaluate the response to treatment in solid tumors. *J Natl Cancer Inst.* 2000;92:205–216.
26. Yip D, Herper PG. Predictive and prognostic factors in small cell lung cancer: current status. *Lung Cancer.* 2000;28:173–185.
27. Thomas CR, Giroux DJ, Janaki LM, et al. Ten year follow up of Southwest Oncology Group 8269: a phase □□□□ trial of concomitant cisplatin-etoposide and daily thoracic radiotherapy in limited small-cell lung cancer. *Lung Cancer.* 2001; 33:213–219.

Mechanisms of action of rapamycin in gliomas[1]

Amy B. Heimberger,[2] Enze Wang, Eric C. McGary, Kenneth R. Hess, Verlene K. Henry, Tadahisa Shono, Zvi Cohen, Joy Gumin, Raymond Sawaya, Charles A. Conrad, and Frederick F. Lang

Brain Tumor Center and Departments of Neurosurgery (A.B.H., E.W., V.K.H., T.S., Z.C., J.G., R.S., F.F.L.), Biostatistics (K.R.H.), and Neuro-Oncology (C.A.C.), The University of Texas M.D. Anderson Cancer Center, Houston, TX 77030; Hilton Head Regional Medical Center, Hilton Head, SC 29926 (E.C.M.); USA

Rapamycin has previously been shown to be efficacious against intracerebral glioma xenografts and to act in a cytostatic manner against gliomas. However, very little is known about the mechanism of action of rapamycin. The purpose of our study was to further investigate the in vitro and in vivo mechanisms of action of rapamycin, to elucidate molecular end points that may be applicable for investigation in a clinical trial, and to examine potential mechanisms of treatment failure. In the phosphatase and tensin homolog deleted from chromosome 10 (PTEN)-null glioma cell lines U-87 and D-54, but not the oligodendroglioma cell line HOG (PTEN null), doses of rapamycin at the IC_{50} resulted in accumulation of cells in G_1, with a corresponding decrease in the fraction of cells traversing the S phase as early as 24 h after dosing. All glioma cell lines tested had markedly diminished production of vascular endothelial growth factor (VEGF) when cultured with rapamycin, even at doses below the IC_{50}. After 48 h of exposure to rapamycin, the glioma cell lines (but not HOG cells) showed downregulation of the membrane type–1 matrix metalloproteinase (MMP) invasion molecule. In U-87 cells, MMP-2 was downregulated, and in D-54 cells, both MMP-2 and MMP-9 were downregulated after treatment with rapamycin. Treatment of established subcutaneous U-87 xenografts in vivo resulted in marked tumor regression ($P < 0.05$). Immunohistochemical studies of subcutaneous U-87 tumors demonstrated diminished production of VEGF in mice treated with rapamycin. Gelatin zymography showed marked reduction of MMP-2 in the mice with subcutaneous U-87 xenografts that were treated with rapamycin as compared with controls treated with phosphate-buffered saline. In contrast, treatment of established intracerebral U-87 xenografts did not result in increased median survival despite inhibition of the Akt pathway within the tumors. Also, in contrast with our findings for subcutaneous tumors, immunohistochemistry and quantitative Western blot analysis results for intracerebral U-87 xenografts indicated that there is not significant VEGF production, which suggests possible deferential regulation of the hypoxia-inducible factor 1α in the intracerebral compartment. These findings demonstrate

Received April 29, 2004; accepted June 29, 2004.

[1] Supported by The University of Texas M.D. Anderson Cancer Center National Institutes of Health Core Grant P30 CA16672, the Bullock Research Foundation, and the Elias Family Fund for Brain Tumor Research.

[2] Address correspondence to Amy B. Heimberger, Department of Neurosurgery, The University of Texas M.D. Anderson Cancer Center, Unit 442, 1515 Holcombe Boulevard, Houston, TX 77030-4009, USA (aheimber@mdanderson.org).

[3] Abbreviations used are as follows: BSA, bovine serum albumin; CD3, T cell type I transmembrane protein; EDTA, ethylenediamine tetraacetic acid; ELISA, enzyme-linked immunosorbent assay; FCS, fetal calf serum; FRAP, FKBP-rapamycin-associated protein; HIF, hypoxia-inducible factor; IC_{50}, inhibitory concentration 50; IL-2, interleukin 2; MMP, matrix metalloproteinase; MT1, membrane type–1; mTOR, mammalian target of rapamycin; PAGE, polyacrylamide gel electrophoresis; PI3K, PI3 kinase; PBS, phosphate-buffered saline; PTEN, phosphatase and tensin homolog deleted from chromosome 10; SDS, sodium dodecyl sulfate; SPF, sterile, pathogen free; VEGF, vascular endothelial growth factor.

[4] Personal communication, Candelaria Gomez-Manzano, M.D. Anderson Cancer Center, September 15, 2004.

that the complex operational mechanisms of rapamycin against gliomas include cytostasis, anti-VEGF, and anti-invasion activity, but these are dependent on the in vivo location of the tumor and have implications for the design of a clinical trial. *Neuro-Oncology 7, 1–11, 2005 (Posted to Neuro-Oncology [serial online], Doc. 04-042, November 17, 2004. URL http://neuro-oncology.mc.duke.edu; DOI: 10.1215/S1152851704000420)*

Classic phase 1 and 2 clinical trials determine the safety and efficacy of agents by evaluating indirect end points based on clinical assessments of toxicity and response, respectively. Reliance on these indirect end points leaves unanswered important questions such as whether the drug actually reaches the tumor and whether it alters the biology of the tumor. Consequently, investigators have proposed revising the standard clinical design of brain tumor trials to also include assessments of molecular targets to optimize dose and to determine efficacy (Lang et al., 2002). For these trials to be successful, however, preclinical studies must be aimed at defining the appropriate molecular end points and developing clinically applicable assays to assess these end points (Lang et al., 2002). A molecular approach makes more efficient use of animal studies given the frequent observation that efficacy in animals only rarely correlates with efficacy in humans. Because several groups have proposed evaluating rapamycin, or one of its derivatives, as a potential treatment for patients with malignant gliomas, we explored the molecular targets of rapamycin in order to determine which ones could be used as end point(s) in molecular target–based, early-phase clinical trials.

Rapamycin has been recognized as an antineoplastic agent and is a potent inhibitor of tumor cell growth (Sehgal et al., 1975; Supko and Malspeis, 1994), specifically inhibiting the Ser-Thr kinase activity of mammalian target of rapamycin (mTOR)[3] FKBP-rapamycin-associated protein (FRAP) (Neshat et al., 2001; Price et al., 1992), a signaling molecule that links extracellular signaling to protein translation (Dilling et al., 1994). Activation of growth factor or cytokine receptors results in the sequential activation of PI3 kinase (PI3K), PDK1, Akt/PKB, and mTOR-FRAP. Treatment of cells with rapamycin leads to the dephosphorylation and inactivation of p70S6 kinase and 4EBP1. Dephosphorylation of 4EBP1 results in the binding to e1F4E, which inhibits translation. The tumor suppressor phosphatase and tensin homolog deleted from chromosome 10 (PTEN) downregulates Akt activity, and PTEN-null cell lines expressing high levels of Akt, such as U-87, U-251, SF-539, and SF-295, are sensitive to rapamycin inhibition of mTOR-FRAP at an IC_{50} of less than 0.01 μM in vitro (Neshat et al., 2001). Although in established subcutaneous U-87 glioma tumors, doses of rapamycin that inhibit mTOR (1 mg/kg administered i.p. once every 3 days) are insufficient for suppression of growth (Eshleman et al., 2002), higher doses of rapamycin (1.5 mg/kg administered i.p. once daily) inhibit tumor growth and angiogenesis (Guba et al., 2002). Furthermore, rapamycin has been shown to be efficacious against established intracerebral U-251 gliomas in a murine model. Specifically, mice treated with rapamycin intraperitoneally at 200, 400, and 800 mg/kg/injection had increased life spans of 67%, 47%, and 78%, respectively, compared to survival of untreated controls (Houchens et al., 1983), suggesting that rapamycin may be a promising agent against gliomas.

The purpose of our study was to further investigate the in vitro and in vivo mechanisms of action of rapamycin in order to elucidate molecular end points that may be applicable in early phase clinical trials and to examine potential mechanisms of treatment failure. This study demonstrates that rapamycin affects cytostasis, cell signaling, angiogenesis, and invasion in vitro. Although rapamycin in our model system demonstrated in vivo efficacy in the subcutaneous compartment, an increase in median survival was not seen in the intracerebral compartment, which indicates that the anatomical microenvironment influences the tumor response to rapamycin.

Materials and Methods

Tumor Cell Lines

The cell lines U-87, D-54, and HOG (provided for our study as a gift) are PTEN null and were maintained in Dulbecco's Modified Eagle Medium/F12 medium (Mediatech, Inc., Herndon, Va.) supplemented with 10% fetal bovine serum (GIBCO-BRL, Rockville, Md.). All cell lines tested negative for *Mycoplasma* contamination. Both U-87 and D-54 express high constitutive levels of hypoxia-inducible factor (HIF)-1α,[4] resulting in enhanced expression of vascular endothelial growth factor (VEGF).

Drugs

Rapamycin (sirolimus; Sigma Chemical Co., St. Louis, Mo.) and its derivative RAD001 [everolimus; 40-O-(2-hydroxyethyl)-rapamycin; Novartis Institutes of Biomedical Research, Novartis Pharma AG, Basel, Switzerland] were stored at a concentration of 5 mg/ml and 10^{-2} M, respectively, in 100% ethanol at –20°C and were diluted in serum-free medium immediately prior to use. The oral formulation of RAD001 is provided as a microemulsion preconcentrate that has efficacy after oral dosing equivalent to that of rapamycin and has the same mode of action at the cellular and molecular level as rapamycin (Schuler et al., 1997). When compared to rapamycin, the in vitro activity of RAD001 is generally about two to three times lower (Schuler et al., 1997).

Murine Models and Tumor Formation

All animal studies were conducted with a protocol approved by the Institutional Animal Care and Use Committees. Male 6- to 8-week-old nude mice (The Jackson Laboratory, Bar Harbor, Maine) were housed within an approved specific pathogen–free barrier facility maintained at the M.D. Anderson Isolation Facility in accordance with Laboratory Animal Resources Com-

mission standards. Appropriate measures were taken to minimize animal discomfort, and appropriate sterile surgical techniques were utilized in tumor implantation and drug administration. Animals that became moribund or had necrotic tumors were compassionately euthanized.

To induce the subcutaneous tumors, logarithmically growing U-87 cells were injected into the right hind flank of nude mice at a dose of 1×10^6 cells per 200 μl. Treatment with rapamycin intraperitoneally at a dose of 1.5 mg/kg/day was begun when the majority of animals had palpable tumors (at day 5). Tumors were measured every other day, and tumor volumes (length × width^2/2) were calculated on the basis of the tumors that grew in surviving mice.

To induce intracerebral tumor, U-87 cells (5×10^5) were engrafted into the caudate nucleus of athymic mice as previously described (Lal et al., 2000). We performed three independent experiments using 6 to 10 animals per group in each experiment. For the survival studies, treatment was started on day 3 after implantation of the U-87 cells, and mice were treated via oral gavage with RAD001, the derivative of rapamycin. To obtain tumors of sufficient size to perform the biological assays, treatment was started on day 7 after implantation of U-87 cells.

In Vitro Cytotoxicity

Cells in logarithmic growth at 80% confluency were harvested with trypsin-EDTA (0.5–0.2 g/liter) solution (GIBCO-BRL), washed with phosphate-buffered saline (PBS), and plated in triplicate in 96-well U-bottom plates at a concentration of 2×10^4 cells/ml. Rapamycin was added at concentrations of 0, 0.001, 0.01, 0.1, 1.0, 10, 100, and 1000 ng/ml, and the plates were incubated at 38°C for 24 h. Counts of viable cells were determined by the trypan blue dye exclusion method.

Cell Cycle Analysis

Cells in logarithmic growth at a concentration of 1.5×10^6 cells/ml were treated with rapamycin at doses of 0, 0.1, 1.0, and 10 ng/ml for U-87 cells; 0, 1.0, 10, and 100 ng/ml for D-54 cells; and 0, 100, and 1000 ng/ml for HOG cells. Cells were fixed with 70% ethanol, stained with 20 μg/ml of propidium iodide and 100 μg/ml of RNase A, and incubated at 37°C for 30 min. Flow cytometric analysis was performed with appropriate gating on a FACScan (Becton Dickinson Immunocytometry Systems, San Jose, Calif.).

Western Blot Analysis

Cell lines or minced tumor tissue underwent protein extraction in 20 mM Tris-HCl, pH 8.0, 137 mM NaCl, 10% glycerol, 0.1% sodium dodecyl sulfate (SDS), leupeptin 0.2 μg/ml, aprotinin 5 μg/ml, phenylmethyl sulfonyl fluoride 1 mM (Sigma), and 1% NP-40 (Amersham, Piscataway, N.J.) for 15 min at 4°C. The supernatant was stored at –70°C after centrifugation. Protein concentration was determined by standard Bio-Rad protein assay (Bio-Rad, Hercules, Calif.). Equivalent amounts of protein extracts (20 μg/well) were subjected to 12.5% SDS–polyacrilamide gel electrophoresis (PAGE) gel denaturing conditions and were immunoblotted with anti-VEGF (Sigma), anti–matrix metalloproteinase 2 (MMP-2) (Sigma), anti-4EBP1 (Cell Signaling Technology, San Jose, Calif.), anti-α-tubulin (Sigma), or anti-β-actin (Sigma). Fold increases in intensity of each band were scanned with a densitometer (Molecular Dynamics, Piscataway, N.J.), normalized to control β-actin or α-tubulin, and analyzed by using ImageQuant (Molecular Dynamics).

Vascular Endothelial Growth Factor Enzyme-Linked Immunosorbent Assay

The glioma cells were treated with rapamycin in serum-free medium as previously described. Cell viability at the completion of the experiment was determined by trypan blue exclusion. The medium was collected and stored at –80°C and was not subjected to more than one freeze-thaw cycle prior to use. VEGF secretion was measured in duplicate samples by enzyme-linked immunosorbent assay (ELISA) according to the manufacturer's instructions (R & D Systems, Minneapolis, Minn.).

Immunohistochemistry

Tumors removed from nude mice were fixed in 10% formalin solution for approximately 6 h at room temperature and then embedded in paraffin. Sections of paraffin-embedded tumors were deparaffinized in xylene, rehydrated, and then stained after endogenous peroxidase was inactivated by treating them with 3% H_2O_2 for 5 min at room temperature. Tissue staining was performed with the HRB-DAB system (R & D Systems) according to the manufacturer's instructions. The primary antibodies utilized were mouse anti-human VEGF (R & D Systems) at a 1:50 dilution or mouse anti-human membrane type–1 (MT1)-MMP (R & D Systems) at a 1:22 dilution. The slides were counterstained with hematoxylin, and the tumor sections were examined with a Nikon microscope.

Gelatin Zymography

The supernatant from glioma cell lines treated with medium containing rapamycin or medium alone was harvested and stored at –80°C prior to use. The samples (each containing 15 μg of supernatant protein) were fractionated by electrophoresis on a polyacrylamide gel containing 10% SDS and gelatin (Bio-Rad). To determine in vivo MMP activity, tumor fragments (10 mm^3 each) were cut from the tumor, weighed, and extracted with 2 × SDS sample buffer (1:2 w/v). After extraction for 2 h at room temperature, samples were diluted 2-fold with 1 × SDS sample buffer and homogenized by repeated pipetting. The solubilized material was separated from the pellet by centrifugation at 14,000 × *g* for 30 min, and aliquots of these supernatants were analyzed by gelatin zymography (20 μl/sample lane). Coo-

massie blue staining confirmed equivalent protein loading of samples on gels.

SDS was subsequently removed from the gels with 2.5% Triton X-100, and they were incubated overnight at 37°C in a solution containing 50 mM Tris base, 200 mM NaCl, 5 mM $CaCl_2$, and 0.02% Brij-35 (30%). The gels were then stained with 0.5% Coomassie blue in 40% methanol and 10% acetic acid for 2 h at room temperature with agitation and then destained with 40% methanol and 10% acetic acid to reveal clear bands of proteolytic activity.

MT1-MMP Analysis

Cell lines treated as previously described with rapamycin or media alone were washed with PBS containing 1% bovine serum albumen (BSA) and stained for 40 min with 10 μg/ml of rabbit control IgG or an antibody against the hinge domain of MT1-MMPs (Sigma). After washing, the cells were stained with the secondary fluorescein isothiocyanate–conjugated $F(ab')_2$ fragment of goat anti-rabbit IgG (Sigma) for 30 min. Cells were analyzed on a Becton Dickinson FACScan with cell population gates for negative control set by using cells stained with rabbit IgG.

Cell Invasion Assay

Tumor cell invasion was measured with Matrigel Invasion Chambers (BD Biosciences, San Jose, Calif.). The glioma cell lines in 5% fetal calf serum (FCS) were added at a concentration of 5×10^4 to the upper chamber, and 10% FCS was used in the lower chamber to induce cell migration. Rapamycin was added to the upper chamber at concentrations spanning the IC_{50}. Duplicate filters were used for each treatment, and all the cells on each filter were counted by using an inverted microscope.

Statistical Analysis

Spearman rank correlation coefficient analysis was used to analyze the VEGF ELISA data. A linear model relating the VEGF values to log dose, time, and cell line was used to include a three-way interaction as well as all nested two-way interactions. Residual analyses demonstrated that the model fit the data. A two-sample *t* test assuming equal variances between groups was used to determine the statistical significance on quantitative Western blot densitometry. The nonparametric Wilcoxon rank sum test was used to compare the volumes of subcutaneous tumors between rapamycin-treated and untreated groups. Statistical significance was determined as $P < 0.05$.

Results

In Vitro Studies

Determination of IC_{50} of rapamycin for glioma cell lines. To determine whether there was a direct cytostatic effect of rapamycin on the growth of U-87, D-54, and HOG cells, these lines in logarithmic growth were exposed to 0 to 1000 ng/ml of rapamycin. After 24 h, the cells were harvested and counted; the IC_{50} for U-87, D-54, and HOG was 0.65, 75, and >1000 ng/ml of rapamycin, respectively.

Table 1. Flow cytometric analysis results showing rapamycin-induced G_1 arrest in D-54 and U-87 glioma cells but not in HOG oligodendroglioma cells*

Cell Line	Time	Rapamycin Dose (ng/ml)	% Sub-G_0/G_1	% G_1	% G_2	% S
D-54	24	0	<1	52.4	10.7	36.9
D-54	24	100	<1	64.3	9.4	26.2
D-54	48	0	<1	40.3	16.1	43.6
D-54	48	10	<1	68.1	5.6	26.4
U-87	24	0	<1	47.0	8.2	44.7
U-87	24	1	<1	59.2	32.3	8.5
U-87	48	0	<1	57.7	25.1	17.2
U-87	48	100	<1	67.8	24.4	7.8
HOG	24	0	<1	38.3	31.1	30.6
HOG	24	1000	<1	35.2	27.2	37.6
HOG	48	0	<1	55.1	28.7	16.2
HOG	48	1000	<1	52.6	26.8	20.6

* Cell lines were treated with rapamycin at the IC_{50} for 24 h, the DNA content was measured by flow cytometry after cells were stained with propidium iodide, and the proportions of cells in G_1, G_2, and S phases of the cell cycle were computed. The experiment was replicated twice at two different time points with similar results.

Rapamycin induces G_1 arrest in glioma cell lines. To determine if rapamycin induced cell cycle arrest, D-54, U-87, and HOG cell lines were treated for 24 and 48 h with medium alone or with medium containing rapamycin at the respective IC_{50} dose determined for each line. Flow analysis cytometry was performed to determine the fraction of cells in subG_0/G_1 (apoptosis), G_1, G_2, and S phases (Table 1). Treatment of the D-54 and U-87 cell lines with rapamycin resulted in the accumulation of cells in the G_1 compartment, indicating that rapamycin acts in a cytostatic manner. Treatment of the HOG cell line, even with maximum doses of rapamycin, failed to induce cytostasis.

RAD001 (everolimus) suppresses the phosphorylation of p-4EBP1, a downstream signal molecule of the Akt pathway. To determine whether the rapamycin derivative RAD001 could decrease the phosphorylation of the downstream signaling molecule p-4EBP1 of the Akt pathway, U-87 cells were cultured for 24 h with doses of RAD001 spanning the IC_{50}, and the amount of p-4EBP1 was quantitated on Western blot. With volumetric band density normalized to a maintenance protein (α-tubulin), RAD001 significantly diminished production of p-4EBP1 (Fig. 1A). This data is consistent with previously published reports that the Akt pathway is inhibited by rapamycin.

Rapamycin suppresses the secretion of VEGF in glioma cell lines. To determine whether rapamycin could

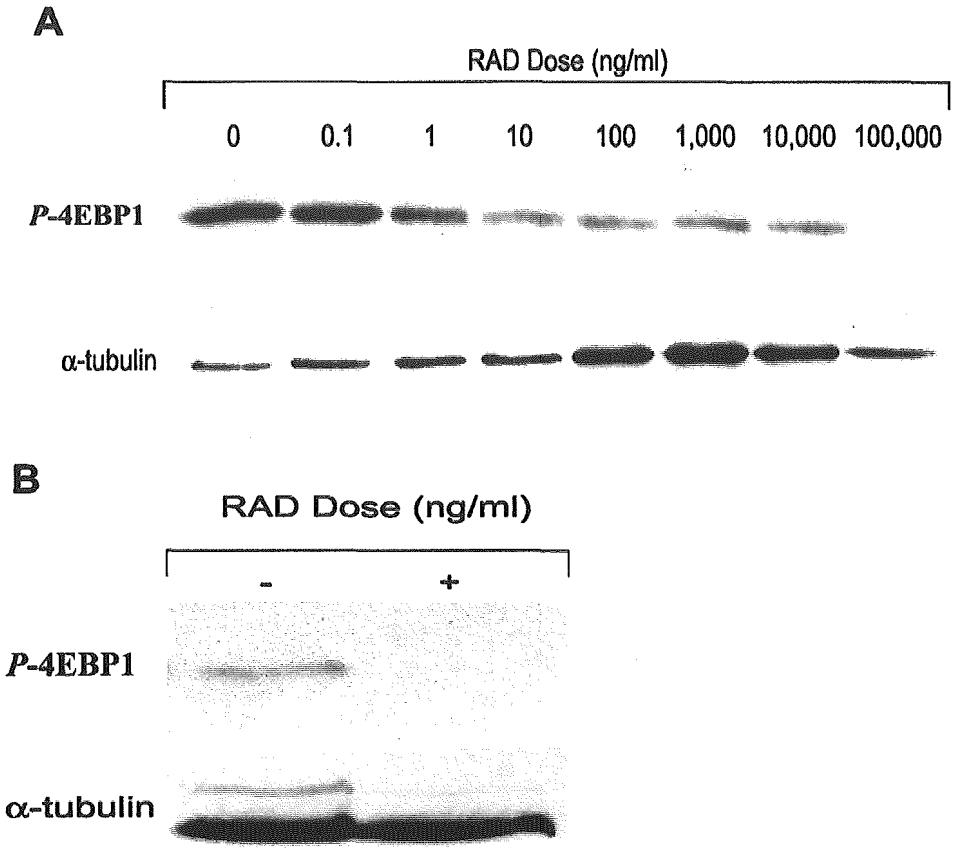

Fig. 1. Quantitative Western blot analysis demonstrating inhibition of p-4EBP1 by RAD001. U-87 (A) or U-87 intracerebral tumors (B) were treated with the derivative of rapamycin, RAD001, as described in the Materials and Methods section. Equivalent amounts of protein extracts (20 μg/well) were subjected to 12.5% SDS-PAGE gel denaturing conditions and were immunoblotted with anti-4EBP1 and anti-α-tubulin. Fold increases in intensity of each band were scanned with a densitometer and normalized to control α-tubulin. RAD001 inhibited the phosphorylated form of 4EBP1, the downstream signaling molecule of Akt, both in vitro and in vivo.

decrease the production of VEGF in vitro, we cultured glioma cells for 24 and 48 h with doses of rapamycin spanning the IC_{50}, and we determined the VEGF concentration by ELISA. To control for the effect of diminished cell number as the basis for diminished VEGF production, cell counts at each time point were determined, and VEGF secretion per cell was calculated. At 24 and 48 h there was a markedly diminished production of VEGF by all glioma cell lines at rapamycin doses significantly below the IC_{50}. Even though an IC_{50} could not be determined for the HOG cell line, dramatic inhibition of VEGF production was seen after 48 h of exposure to rapamycin at 10 ng/ml (Fig. 2).

Rapamycin inhibits invasion and downregulates MMPs. The enzymatic activities of MT1-MMP and MMP-2 contribute to the integrity of the extracellular matrix in the brain, and hydrolysis of the brain's extracellular matrix allows glioma cells to invade normal brain tissue. To determine whether rapamycin downregulates MMPs, we treated the cell lines U-87, D-54, and HOG in vitro with rapamycin for 48 h, and we used flow cytometry to quantify the amount of the membrane-bound MMP, MT1-MMP, after the cell line had been exposed to a monoclonal antibody to MT1-MMP (see Materials and Methods). After 48 h of treatment with 10 ng/ml and 100 ng/ml of rapamycin, respectively, the glioma cell lines U-87 and D-54 showed downregulation of MT1-MMP (Table 2). In contrast, there were minimal levels of MT1-MMP expressed in the HOG cell lines, which did not appear to be affected by treatment with 1000 ng/ml of rapamycin (data not shown).

Because MT1-MMP-expressing glioma cells can activate proMMP-2, with the resulting enzymatic activity of MMP-2 facilitating tumor invasion of normal brain, we determined if rapamycin downregulated the secretory invasion molecules MMP-2 and MMP-9. The glioma cell lines were treated with rapamycin for 48 h, and for each cell line, the supernatant was harvested, the protein was quantitated, and gelatin zymography was performed. In the U-87 glioma line, the invasion molecule MMP-2 was downregulated by treatment with 10 ng/ml

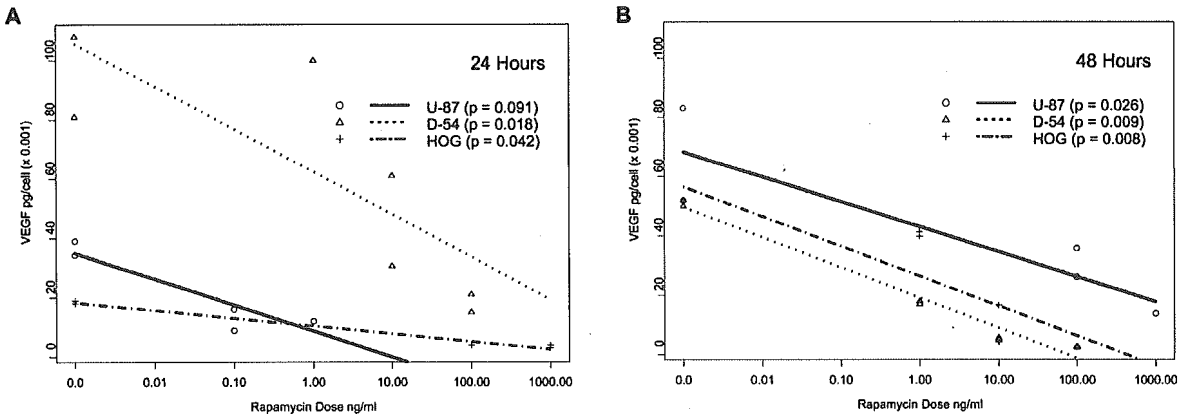

Fig. 2. Downregulation of VEGF in rapamycin-treated glioma cells. Glioma cell lines (D-54 and U-87) and HOG oligodendroglioma cells were treated with the indicated doses of rapamycin for 24 h (panel A) and 48 h (panel B), and their VEGF production was determined by ELISA assay. Diminished cell numbers were accounted for by calculating VEGF production per viable cell. The experiment was replicated in duplicate samples over two different time points with similar outcomes. A linear model relating the VEGF values to log dose, time, and cell line was used to include a three-way interaction as well as all nested two-way interactions. Residual analyses demonstrated that the model fit the data. The *P*-value for the three-way interaction was 0.05, that for the two-way interaction between dose and time was 0.47, that for dose and cell line was 0.033, and that between time and cell line was <0.0001.

of rapamycin; however, significant quantities of MMP-9 were not present in untreated cells. In the D-54 cell line, both MMP-2 and MMP-9 were present and downregulated by 100 ng/ml of treatment with rapamycin. In the HOG cell line, only MMP-2 was present, and it did not appear to be altered by treatment with 1000 ng/ml of rapamycin (Fig. 3).

To determine if rapamycin inhibits in vitro invasion, glioma cell lines were treated with rapamycin for 24 h. In the U-87 and D-54 cell lines, invasion was inhibited with rapamycin concentrations below the IC_{50}. In contrast, in the HOG cell line, even treatment with 1000 ng/ml of rapamycin failed to alter in vitro invasion (Fig. 4).

In Vivo Studies: Subcutaneous Model

Rapamycin suppresses growth of subcutaneous tumors. To determine if rapamycin was efficacious in the treatment of established tumors, subcutaneous U-87 tumors were treated with 1.5 mg/kg/day of rapamycin for 45 days. In 63% (n = 8) of established tumors treated with rapamycin, there was regression with no evidence of residual tumor at the conclusion of the experiment. In all U-87 tumors treated with PBS alone (n = 8), there was no evidence of regression, and all mice had large tumors at the conclusion of the experiment ($P < 0.05$) (Fig. 5).

Rapamycin inhibits in vivo VEGF. To verify that rapamycin downregulates VEGF production in vivo, we treated subcutaneous U-87 tumors for 45 days with 1.5 mg/kg/day of rapamycin. Subsequent immunohis-

Table 2. Flow cytometric analysis results showing downregulation of the invasion molecule MT1-MMP by rapamycin on U-87 and D-54 cells*

Cell Line	Rapamycin Dose (ng/ml)	% MTI-MMP Positive Cells
D-54	0	15.6
D-54	100	7.25
U-87	0	9.9
U-87	10	3.45
HOG	0	3.95
HOG	1000	8.43

* The cells were treated for 48 h with rapamycin. The cells were then incubated with an isotype control antibody or an MT1-MMP-specific antibody with an FITC-conjugated fragment of goat anti-rabbit IgG and analyzed by flow cytometry. Positive isotype control staining was less than 1.9%.

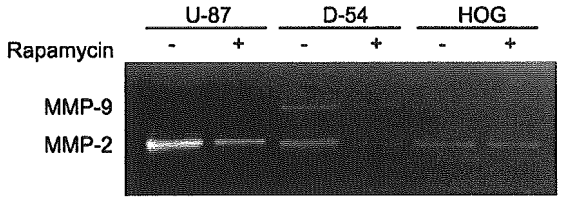

Fig. 3. Gelatin zymograph showing downregulation of the invasion molecules MMP-2 and MMP-9 by rapamycin. The glioma (U-87 and D-54) and oligodendroglioma (HOG) cell lines were treated for 48 h with rapamycin. The supernatant was harvested from each respective cell line, and 15 μg of protein from each supernatant was fractionated by gelatin zymography. Untreated (medium only) U-87 cells express MMP-2 but little MMP-9. U-87 cells treated with 10 ng/ml of rapamycin show MMP-2 downregulation. Untreated (medium only) D-54 cells express both MMP-2 and MMP-9. However, D-54 cells treated with 100 ng/ml of rapamycin demonstrated downregulation of both MMP-2 and MMP-9. Untreated (medium only) HOG cells expressed only MMP-2, and when this cell line was treated with the maximal dose of 1000 ng/ml of rapamycin, there was no change in MMP-2 expression.

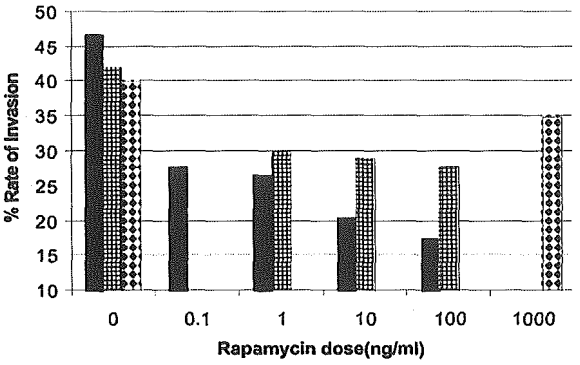

Fig. 4. In vitro invasion assay demonstrating that rapamycin inhibits invasion. U-87, D-54, and HOG cell lines were treated for 24 h with rapamycin. The glioma cells lines in 5% FCS were added at a concentration of 5×10^4 to the upper chamber, and 10% FCS was used in the lower chamber to induce cell migration. Rapamycin was added to the upper chamber at concentrations spanning the IC_{50}. Invasion was inhibited with rapamycin at concentrations less than the IC_{50} in both the U-87 and D-54 cell lines. However, even at 1000 ng/ml, rapamycin did not significantly inhibit the invasion of the HOG cell line. Solid bars, U-87; bars with small squares, D-54; white bars with black diamonds, HOG.

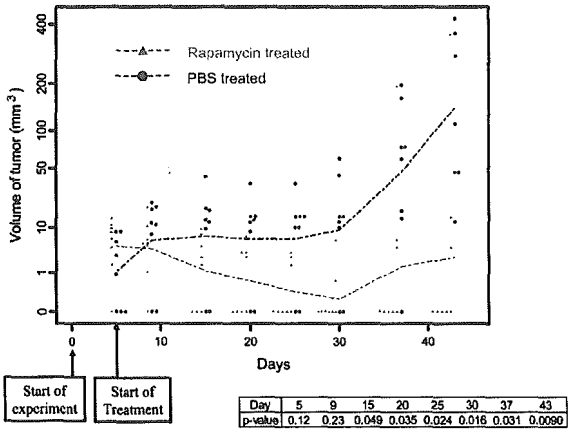

Fig. 5. Changes with time in the volume of subcutaneous U-87 tumors in nude mice with and without rapamycin treatment. Nude mice with established tumors (from subcutaneous injection of U-87 glioma cells) were treated daily with rapamycin at 1.5 mg/kg/day. There was regression in 63% (n = 8) of these tumors, with no evidence of residual tumor at the conclusion of the experiment (day 50) ($P < 0.05$). In contrast, all mice treated with PBS alone (n = 8) had large tumors at the conclusion of the experiment.

tochemical studies demonstrated that there was diminished VEGF production in tumors treated with rapamycin (Fig. 6). Determination of volumetric band density normalized to a maintenance protein (β-actin) on Western blot revealed that VEGF levels in tumors that were treated with rapamycin were lower (mean = 2.2; SD = 1.46) than those in tumors that were treated with PBS (mean = 5.3; SD = 1.27; $P = 0.037$) (Fig. 7). VEGF production did not appear to vary among the various tumor sizes in the PBS treatment group. Interestingly, the one rapamycin-treated U-87 tumor that achieved a size similar to the PBS-treated control tumors had a localized area of diminished VEGF production but had discrete areas of high VEGF production, possibly representing a mechanism of chemotherapy resistance. This tumor remained small volumetrically until day 30, at which point growth increased 60-fold in 15 days.

Rapamycin inhibits in vivo metalloproteinases. To determine if rapamycin modulated MMPs in vivo, subcutaneous U-87 tumors were treated with rapamycin and formalin fixed. Immunohistochemical staining failed to demonstrate dramatic changes in the level of MT1-MMP in U-87 tumors treated in vivo with rapamycin as compared to U-87 tumors treated with PBS. MT1-MMP staining was most prominent at the tumor periphery and appeared slightly more intense in U-87 tumors treated with PBS than in those treated with rapamycin (data not shown). Because MT1-MMP activity is necessary for the activation of proMMP-2, zymography was performed to identify the status of MMP-2 in U-87 tumors. Among rapamycin-treated subcutaneous U-87 tumors large enough to analyze 45 days after tumor implantation (n = 3), there was a marked reduction of MMP-2 (seen by gelatin zymography) as compared with the U-87 tumors treated with PBS alone (Fig. 8). The one rapamycin-treated tumor that escaped growth suppression did not show upregulation of MMP-2. These results are consistent with our in vitro data, thus confirming that rapamycin has an effect on MMPs.

In Vivo Studies: Intracranial Model

RAD001 fails to suppress orthotopic U-87 growth. Secondary to Novartis's interest in proceeding with a clinical trial for patients with malignant gliomas and since rapamycin has previously been demonstrated to be efficacious against established intracerebral xenografts, we elected to determine if RAD001 was efficacious in the treatment of established orthotopic U-87. Tumors were treated with 1.5 mg/kg/day or 5 mg/kg/day of the derivative of rapamycin, RAD001, starting three days after intracerebral implantation. In mice (n = 10/group) treated with 5 mg/kg or 1.5 mg/kg of RAD001 or with diluent, median survival was 30.5, 30.5, and 31 days, respectively, which was not statistically significant (data not shown). Three separate experiments produced similar results.

On quantitative Western blot analysis of orthotopically implanted U-87 tumors treated with RAD001, there was diminished p-4EBP1 (Fig. 1B). On immunohistochemistry, there was no discernable VEGF production within the intracerebral U-87 tumors, nor was there a difference with RAD001 treatment. Furthermore, Western blot analysis confirmed that there was no significant change in VEGF production. The intracerebral U-87 tumors treated with RAD001 demonstrated no significant changes in MMP-2 production on quantita-

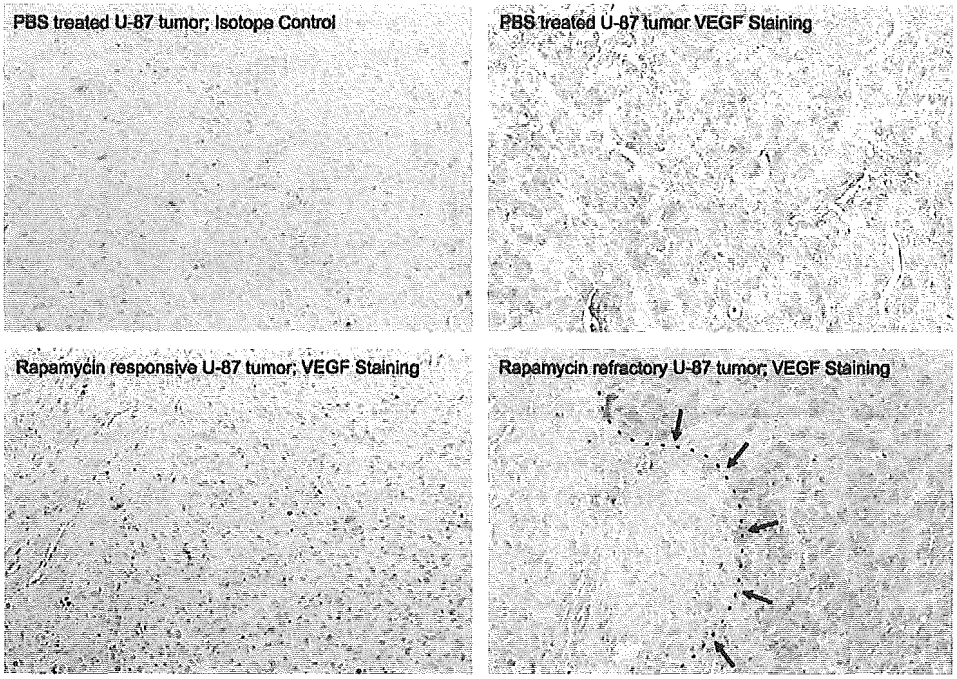

Fig. 6. Diminished immunohistochemical staining for vascular endothelial growth factor in subcutaneous U-87 cell tumors in nude mice after rapamycin treatment. Nude mice with established subcutaneous U-87 cell tumors were treated with rapamycin, and after 45 days of treatment, the experiment was terminated and the tumors were harvested. Paraffin-embedded sections of the tumors were stained with anti-VEGF antibody, and visualization employed the strepavidin-horseradish peroxidase system. In the lower right-hand panel, in the only U-87 tumor treated with rapamycin that attained a size similar to control-treated tumors, there was an area that was negative for VEGF staining (denoted by arrows), but the majority of the tumor demonstrated areas of high VEGF production (original magnification × 250).

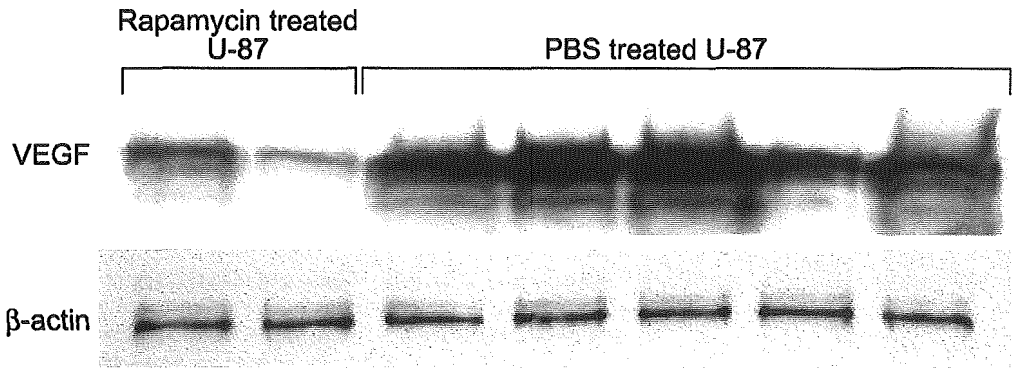

Fig. 7. Quantitative Western blot analysis demonstrating decreased VEGF production in vivo. Nude mice with established tumors (from subcutaneous injection of U-87 glioma cells) were treated daily with rapamycin at 1.5 mg/kg/day, and after 45 days of treatment, the tumors were harvested. The tumors were minced and underwent protein extraction. Equivalent amounts of protein extracts (20 μg/well) were subjected to 12.5% SDS-PAGE gel denaturing conditions and were immunoblotted with anti-VEGF and anti-β-actin. Fold increases in intensity of each band were scanned with a densitometer and normalized to control β-actin. Rapamycin inhibited VEGF production in vivo.

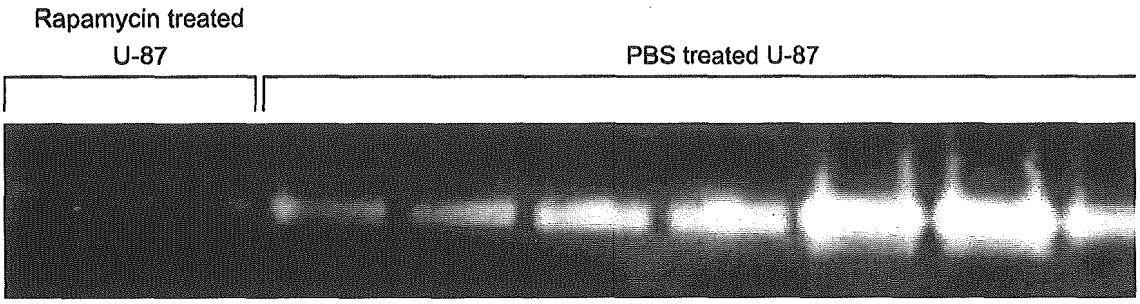

Fig. 8. Gelatin zymograph showing diminished production of MMP-2 in subcutaneous U-87 cell tumors in nude mice after rapamycin treatment. Nude mice with established subcutaneous U-87 cell tumors were treated with rapamycin, and after 45 days of treatment, the experiment was terminated and tumors were harvested. The tumor proteins were extracted and analyzed by gelatin zymography. Few rapamycin-treated U-87 tumors were of sufficient size to analyze (PBS-treated U-87 tumors were large and necrotic), but those that could be analyzed demonstrated diminished MMP-2 expression.

tive Western blot analysis or increased invasion characteristics by histology.

Discussion

One of the purposes of our study was to further elaborate on the mechanism of action of rapamycin so that salient molecular end point(s) could be identified for a clinical trial of rapamycin for glioma patients (Fig 9). These end points could include cytostasis, cell signaling, angiogenesis, and invasion. In this study we show that rapamycin or its derivative RAD001 not only works as a cytostatic agent by the accumulation of cells in the cell cycle G_1 compartment, with a corresponding decrease in the fraction of cells traversing the S phase, but also as an antiangiogenic (by inhibiting VEGF secretion) and an anti-invasion agent (by downregulating MT1-MMP, MMP-2, and MMP-9). Our data is consistent with findings of previously published studies indicating that mTOR-FRAP can regulate the activity of VEGF and invasion. Specifically, the signaling molecule mTOR-FRAP has previously been shown to be an upstream activator of HIF-1 (Hudson et al., 2002), and insulin has been shown to regulate HIF-1 action through PI3K/TOR-dependent pathways (Treins et al., 2002). The binding of HIF-1α to the VEGF promoter is a predominant enhancer of VEGF production (Fang et al., 2001; Tsuzuki et al., 2000), and rapamycin has been shown to inhibit the in vitro and in vivo production of VEGF (Brugarolas et al., 2003; El-Hashemite et al., 2003). In a recent article by Guba et al., rapamycin was shown to inhibit subcutaneous syngeneic adenocarcinomas by acting as an antiangiogenic agent by specifically inhibiting VEGF (Guba et al., 2002). Our studies confirm that downregulation of VEGF by rapamycin occurs in gliomas as well. In the VEGF ELISA, there was markedly diminished production of VEGF in all glioma cell lines, including the HOG cell line, in which rapamycin did not act in a cytostatic manner. Moreover, VEGF production was inhibited at rapamycin doses lower than the IC_{50}.

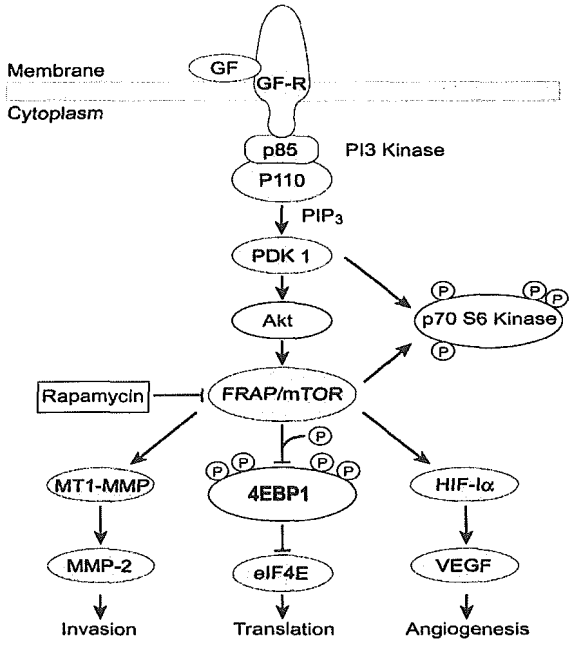

Fig. 9. Molecular targets of rapamycin. Activation of growth factor (GF) or cytokine receptors results in the sequential activation of PI3K, PDK1, Akt/PKB, and mTOR-FRAP. The tumor suppressor PTEN downregulates Akt activity (not shown). Rapamycin treatment of cells leads to the dephosphorylation (denoted by an encircled P) and inactivation of p70S8 kinase and 4EBP1. The dephosphorylation of 4EBP1 results in binding to eIF4E, which inhibits translation. Furthermore, the inhibition of mTOR-FRAP results in downregulation of HIF-1α and subsequent VEGF production. Finally, the inhibition of mTOR-FRAP also results in the downregulation of MT1-MMP, subsequent MMP-2 production, and resulting invasion.

Furthermore, in subcutaneous U-87 tumors, treatment with rapamycin resulted in diminished production of VEGF.

VEGF has been shown to upregulate several invasion molecules, such as MMP-2, MMP-9, and MT1-MMP (Rooprai et al., 2000), and insulin-like growth factor-1 has been shown to regulate MMP-2 and its MT1-MMP-mediated activation by the PI3K/Akt/mTOR pathway (Zhang and Brodt, 2003). In the U-87 and D-54 glioma cell lines, the invasion molecule MMP-2 and both MMP-2 and MMP-9, respectively, were downregulated with rapamycin. Additionally, flow cytometric analysis showed downregulation of MT1-MMP in U-87 and D-54 after 48 h of treatment. Treatment of the subcutaneous U-87 tumors with rapamycin in vivo also resulted in the downregulation of MMP-2. Therefore, treatment with rapamycin in vitro and in the subcutaneous model results in a cytostatic response with downregulation of MMPs and VEGF.

In contrast to the inhibition of tumor growth with rapamycin in the subcutaneous model, mice with established intracerebral U-87 tumors that were treated with RAD001 showed no increase in median survival. Our findings are in contrast to previously published data, which demonstrated a significant increase in median survival of mice with established intracerebral U-251 cells treated with rapamycin (Houchens et al., 1983). These differences may be secondary to as-yet-undefined differences between rapamycin and RAD001 or differences in the tumor models. The difference in efficacy in the subcutaneous and intracerebral models may be secondary to the intracerebral microenvironment, possibly due to influences on hypoxic response and neovascularization, which influences tumor response. Intratumoral p-4EBP1 was inhibited in those mice treated with RAD001, an indication that the concentrations of RAD001 used in vivo were able to inhibit the Akt pathway. Blouw et al. (2003) have shown that HIF-1α-knockout-transformed astrocytes have diminished growth in the vessel-poor subcutaneous environment resulting in severe necrosis as well as reduced growth and vessel density, whereas cells of the same type that are placed into the vascular-rich brain parenchyma have enhanced growth and invasion. Our data is consistent with this previously published report. By immunohistochemistry and quantitative Western blot analysis, the intracerebral U-87 tumors failed to show any appreciable levels of VEGF in vivo, which indicated that additional or alternative mechanisms are involved in VEGF regulation intracerebrally. Although rapamycin may inhibit signal transduction and/or cellular proliferation, the inhibition of HIF-1α may not be a desired strategy to treat astrocytomas since they may adapt to becoming more invasive and infiltrative (Blouw et al., 2003). However, we did not see evidence of increased invasion by histology or upregulation of MMP-2 on Western blot of RAD001-treated intracerebral U-87 tumors. Previously, Houchens et al. demonstrated an increase in median survival in mice with intracerebral U-251 tumors treated with rapamycin, which is in contrast to our data with intracerebral U-87. The difference in results may be, in part, due to differential dosing amount and interval of rapamycin administration, model systems, and/or the underlying molecular status of the tumors.

Given the lack of concordance between murine models and human efficacy, murine model systems are perhaps best utilized for establishing appropriate molecular end points, but these will require validation in human subjects. A proposed clinical trial could begin with a stereotactic biopsy to confirm the diagnosis and establish a baseline of the molecular targets, including p-4EBP1, VEGF, HIF-1α, and MMP-2. After administration of rapamycin or RAD001, the tumor could be removed for analysis of pharmacokinetic and drug-related molecular changes. In the scenario of treatment failure, re-resection or biopsy could establish definitely if failure is occurring through the HIF-1α/VEGF pathway. If this is a mechanism(s) of treatment failure, combination therapy with an anti-VEGF agent may be considered. In conclusion, our data suggest that clinical trials that incorporate only a limited molecular target such as a signal transduction molecule may not necessarily correlate with efficacy and will be inadequate to assess treatment failures and future combination chemotherapeutics.

Acknowledgments

We thank David M. Wildrick for editorial assistance, Hyung-Woo Kim for statistical analysis, and Jeffrey S. Weinberg and Mark R. Gilbert for thoughtful commentary. The oligodendroglioma cell line, HOG, was provided through the courtesy of Ken Aldalpe of The University of Texas M.D. Anderson Cancer Center.

References

Blouw, B., Song, H., Tihan, T., Bosze, J., Ferrara, N., Gerber, H.P., Johnson, R.S., and Bergers, G. (2003) The hypoxic response of tumors is dependent on their microenvironment. *Cancer Cell* **4**, 133–146.

Brugarolas, J.B., Vazquez, F., Reddy, A., Sellers, W.R., and Kaelin, W.G., Jr. (2003) TSC2 regulates VEGF through mTOR-dependent and -independent pathways. *Cancer Cell* **4**, 147–158.

Dilling, M.B., Dias, P., Shapiro, D.N., Germain, G.S., Johnson, R.K., and Houghton, P.J. (1994) Rapamycin selectively inhibits the growth of childhood rhabdomyosarcoma cells through inhibition of signaling via the type I insulin-like growth factor receptor. *Cancer Res.* **54**, 903–907.

El-Hashemite, N., Walker, V., Zhang, H., and Kwiatkowski, D.J. (2003) Loss of Tsc1 or Tsc2 induces vascular endothelial growth factor production through mammalian target of rapamycin. *Cancer Res.* **63**, 5173–5177.

Eshleman, J.S., Carlson, B.L., Mladek, A.C., Kastner, B.D., Shide, K.L., and Sarkaria, J.N. (2002) Inhibition of the mammalian target of rapamycin sensitizes U87 xenografts to fractionated radiation therapy. *Cancer Res.* **62**, 7291–7297.

Fang, J., Yan, L., Shing, Y., and Moses, M.A. (2001) HIF-1alpha-mediated up-regulation of vascular endothelial growth factor, independent of basic fibroblast growth factor, is important in the switch to the angiogenic phenotype during early tumorigenesis. *Cancer Res.* **61**, 5731–5735.

Guba, M., von Breitenbuch, P., Steinbauer, M., Koehl, G., Flegel, S., Hornung, M., Bruns, C.J., Zuelke, C., Farkas, S., Anthuber, M., Jauch, K.W., and Geissler, E.K. (2002) Rapamycin inhibits primary and metastatic tumor growth by antiangiogenesis: Involvement of vascular endothelial growth factor. *Nat. Med.* **8**, 128–135.

Houchens, D.P., Ovejera, A.A., Riblet, S.M., and Slagel, D.E. (1983) Human brain tumor xenografts in nude mice as a chemotherapy model. *Eur. J. Cancer Clin. Oncol.* **19**, 799–805.

Hudson, C.C., Liu, M., Chiang, G.G., Otterness, D.M., Loomis, D.C., Kaper, F., Giaccia, A.J., and Abraham, R.T. (2002) Regulation of hypoxia-inducible factor 1alpha expression and function by the mammalian target of rapamycin. *Mol. Cell Biol.* **22**, 7004–7014.

Lal, S., Lacroix, M., Tofilon, P., Fuller, G.N., Sawaya, R., and Lang, F.F. (2000) An implantable guide-screw system for brain tumor studies in small animals. *J. Neurosurg.* **92**, 326–333.

Lang, F.F., Gilbert, M.R., Puduvalli, V.K., Weinberg, J., Levin, V.A., Yung, W.K., Sawaya, R., Fuller, G.N., and Conrad, C.A. (2002) Toward better early-phase brain tumor clinical trials: A reappraisal of current methods and proposals for future strategies. *Neuro-Oncol.* **4**, 268–277.

Neshat, M.S., Mellinghoff, I.K., Tran, C., Stiles, B., Thomas, G., Petersen, R., Frost, P., Gibbons, J.J., Wu, H., and Sawyers, C.L. (2001) Enhanced sensitivity of PTEN-deficient tumors to inhibition of FRAP/mTOR. *Proc. Natl. Acad. Sci. USA* **98**, 10314–10319.

Price, D.J., Grove, J.R., Calvo, V., Avruch, J., and Bierer, B.E. (1992) Rapamycin-induced inhibition of the 70-kilodalton S6 protein kinase. *Science* **257**, 973–977.

Rooprai, H.K., Rucklidge, G.J., Panou, C., and Pilkington, G.J. (2000) The effects of exogenous growth factors on matrix metalloproteinase secretion by human brain tumour cells. *Br. J. Cancer* **82**, 52–55.

Schuler, W., Sedrani, R., Cottens, S., Haberlin, B., Schulz, M., Schuurman, H.J., Zenke, G., Zerwes, H.G., and Schreier, M.H. (1997) SDZ RAD, a new rapamycin derivative: Pharmacological properties in vitro and in vivo. *Transplantation* **64**, 36–42.

Sehgal, S.N., Baker, H., and Vézina, C. (1975) Rapamycin (AY-22,989), a new antifungal antibiotic, II. Fermentation, isolation and characterization. *J. Antibiot. (Tokyo)* **28**, 727–732.

Supko, J.G., and Malspeis, L. (1994) Dose-dependent pharmacokinetics of rapamycin-28-*N*,*N*-dimethylglycinate in the mouse. *Cancer Chemother. Pharmacol.* **33**, 325–330.

Treins, C., Giorgetti-Peraldi, S., Murdaca, J., Semenza, G.L., and Van Obberghen, E. (2002) Insulin stimulates hypoxia-inducible factor 1 through a phosphatidylinositol 3-kinase/target of rapamycin-dependent signaling pathway. *J. Biol. Chem.* **277**, 27975–27981.

Tsuzuki, Y., Fukumura, D., Oosthuyse, B., Koike, C., Carmeliet, P., and Jain, R.K. (2000) Vascular endothelial growth factor (VEGF) modulation by targeting hypoxia-inducible factor-1alpha→ hypoxia response element→ VEGF cascade differentially regulates vascular response and growth rate in tumors. *Cancer Res.* **60**, 6248–6252.

Zhang, D., and Brodt, P. (2003) Type 1 insulin-like growth factor regulates MT1-MMP synthesis and tumor invasion via PI 3-kinase/Akt signaling. *Oncogene* **22**, 974–982.

Full text, figures, and tables are available online at www.neurosurgery-online.com

LATERAL TRANSSULCAL APPROACH TO ASYMPTOMATIC TRIGONAL MENINGIOMAS WITH CORRELATIVE MICROSURGICAL ANATOMY: TECHNICAL CASE REPORT

Shinji Nagata, M.D., Tomio Sasaki, M.D.

Department of Neurosurgery, Kyushu University Graduate School of Medical Sciences, Fukuoka, Japan (SN, TS)

With commentaries from **Evandro P. de Oliveira**, *São Paulo, Brazil;* **M. Gazi Yaşargil**, *Little Rock, AR, and* **Saleem I. Abdulrauf**, *St. Louis, MO;* **Nicolas de Tribolet**, *Geneva, Switzerland;* **Nobuhiro Mikuni** *and* **Nobuo Hashimoto**, *Kyoto, Japan*

OBJECTIVE AND IMPORTANCE: We introduce the lateral transsulcal approach to asymptomatic trigonal meningiomas.

METHODS: The approach was studied in two cadaver brains and three asymptomatic patients with trigonal meningiomas. The posterior part of the sylvian fissure, or superior temporal sulcus, is opened to the bottom. Through a small horizontal cortical incision, the trigone of the lateral ventricle is exposed in the shortest distance. The trigonal meningiomas are detached from the choroid plexus and removed.

RESULTS: In patients with meningiomas on the nondominant side, the transsylvian approach was adopted. In patients with meningiomas on the dominant side, the transsylvian approach was adopted for patients with a wide sylvian cistern, and the approach through the superior temporal sulcus was adopted for patients with a narrow sylvian cistern. The transverse gyrus of Heschl was a good anatomic landmark in the operative field of the transsylvian approach. Patients with meningiomas on the dominant side exhibited transient amnestic aphasia and dyscalculia, but the symptoms disappeared in a few days or weeks. These patients were discharged without any neurological deficits. Although there are potential risks of damaging association fibers, optic radiation, the transverse gyrus of Heschl, and the parietal lobe, a thorough understanding of the topographical anatomy and careful dissection techniques can avoid morbidity. Wide opening of the sylvian fissure and debulking of the tumor are other important factors to reduce the retraction of the parietal and temporal lobes.

CONCLUSION: The lateral transsulcal approach is applicable for small asymptomatic trigonal meningiomas with an acceptable risk of morbidity, even in the dominant hemisphere.

KEY WORDS: Asymptomatic trigonal meningioma, Lateral transsulcal approach, Superior temporal sulcus, Transsylvian approach, Transverse gyri of Heschl

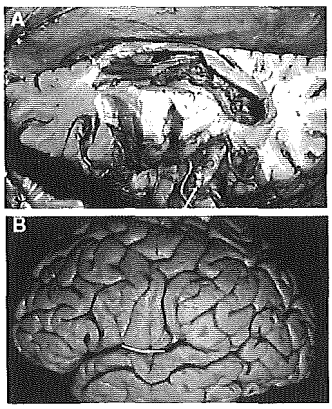

FIGURE 1. *A, cadaveric photograph. In the left cerebral hemisphere of the cadaver brain, the frontal and parietal lobes were removed to show the relationship among the insular cortex, temporal lobe, and trigone of the lateral ventricle. The transverse gyri of Heschl (asterisk) were clearly identified on the superior surface of the temporal lobe. The medial end of the anterior transverse gyrus of Heschl corresponds to the posterior end of the insular cortex, and the longitudinal axis (arrow) corresponds to the access to the trigone of the lateral ventricle. B, the transverse gyrus of Heschl is not observed on the lateral surface of the brain. It corresponds to the sylvian fissure under the somatosensory cortex (white solid line).*

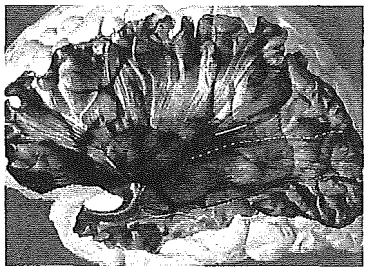

FIGURE 2. *Schematic drawing of the relationship between the optic radiation and the site of the insular incision. The optic radiation (dotted line) runs in the temporal lobe and is separated from the insular incision (solid line).*

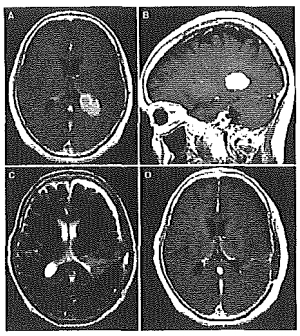

FIGURE 3. *Preoperative and postoperative magnetic resonance images of Patient 3. The preoperative gadolinium diethylenetriamine penta-acetic acid-enhanced images (A and B) show a homogeneously enhanced oval mass of 3.5 cm in maximal diameter at the trigone of the left lateral ventricle. The postoperative gadolinium diethylenetriamine penta-acetic acid-enhanced images 7 days after surgery (C and D) prove the total removal of the trigonal meningioma. There are focal edemas along the surgical access to the trigone.*

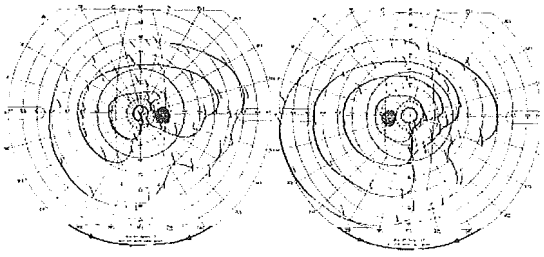

FIGURE 4. *Postoperative scotometry of Patient 1 shows an incomplete left lower quadrantanopia, although the patient noticed no difficulty in daily independent life.*

Neurosurgery 56[ONS Suppl 2]:438, 2005 DOI: 10.1227/01.NEU.0000156553.94932.DD **Received,** June 21, 2004; **Accepted,** November 6, 2004.

Acta Neurochir (Wien) (2005) 147: 863–869
DOI 10.1007/s00701-005-0554-y

Acta Neurochirurgica
Printed in Austria

Neurosurgical Technique

The transsylvian trans-limen insular approach to the crural, ambient and interpeduncular cisterns

S. Nagata and **T. Sasaki**

Department of Neurosurgery, Kyushu University Graduate School of Medical Sciences, Fukuoka, Japan

Received October 20, 2004; accepted April 12, 2005; published online June 3, 2005

Summary

Background. The authors introduce the transsylvian trans-limen insular approach to the crural, ambient and interpeduncular cisterns.

Method. The transsylvian trans-limen insular approach was performed in 7 patients; 3 for aneurysm, 2 for isolated temporal horn hydrocephalus, one for tumour and one for an arteriovenous malformation. This approach is summarized in 4 procedures; the exposure of the inferior limiting sulcus of the insular cortex, the exposure of the inferior horn of the lateral ventricle, the dissection of the inferior part of the choroidal fissure and the splitting of the inferior border of the limen insula.

Findings. Four among 7 patients underwent surgery for the lesions in the crural or ambient cistern. The other 3 patients underwent surgery for the lesion in the interpeduncular cistern. Two patients of the latter group postoperatively had temporal lobe infarction.

Conclusions. The transsylvian trans-limen insular approach may be indicated for lesions in the crural and the anterior ambient cisterns, and the lesions which need wider exposure of the interpeduncular cistern. For the former lesions, this approach can afford good results. For the latter lesions, careful brain retraction and some other techniques to avoid temporal lobe infarction are necessary. Further neuropsychological assessment should be also necessary to prove the validity of this approach.

Keywords: Limen insula; inferior horn of the lateral ventricle; temporal stem; surgical approach.

Introduction

In the pterional approach, the exposure of the crural and anterior part of the ambient cisterns is restricted by the insular cortex. The subtemporal approach can afford a good exposure, however, there are profound risks of temporal lobe contusion and the damage of the bridging vein to the sphenoparietal sinus. By splitting the limen insula at the inferior limiting sulcus, the crural and ambient cisterns can be widely exposed through the pterional access. The incision of the limen insula, however, has the potential risk of damaging the anterior perforated substance and the anterior choroidal artery. Microsurgical anatomy of this area [4–7] will help us to avoid these complications. In this paper, we discuss the clinical application of the transsylvian trans-limen insular approach to the crural, ambient and interpeduncular cisterns.

Methods and materials

We have performed the transsylvian trans-limen insular approach in 7 patients; 3 for ruptured intracranial aneurysm, 2 for isolated temporal horn hydrocephalus, one for suprasellar tumour and one for temporal lobe arteriovenous malformation (Table 1). After thorough exposure of Sylvian cistern through the pterional approach, the inferior limiting sulcus of the insular cortex is exposed. The anterior temporal branches of the middle cerebral artery are dissected free from the surface of the temporal lobe as much as possible. At 2 cm behind the limen insula, a small horizontal incision is made on the inferior limiting sulcus. The incision is advanced to the inferior horn of the lateral ventricle. The choroid plexus is identified first in the inferior horn to make sure the ventricular anatomy. The choroidal fissure, the attachment of the choroid plexus on the wall of the lateral ventricle, is exposed by retracting the choroid plexus superiorly. It is opened to the inferior choroidal point between the choroid plexus and fimbria by cutting the taenia fimbriae. Between the inferior limiting sulcus and the inferior choroidal point, the limen insula is split to expose the crural and the anterior part of the ambient cisterns. The interpeduncular cistern is well exposed through the widely opened crural and ambient cisterns (Fig. 1).

Results

Indications to use the transsylvian trans-limen insular approach

In 3 cases with ruptured intracranial aneurysm (Cases 1–3), one had an aneurysm of the congenital

Table 1. *Clinical features of 7 patients who underwent the transsylvian trans-limen insular approach*

Case	Age/sex	Diagnosis	Preoperative state	Operation	Complication	Outcome
1	41/F	IC-ant.chor.aneurysm	WFNS grade 1	clipping	none	GR
2	71/F	BA-SCA aneurysm	WFNS grade 4	clipping	temporal lobe infarction	SD
3	72/F	BA bif. aneurysm	WFNS grade 4	clipping	none	SD
4	34/F	temporal lobe AVM	alert	total removal	none	GR
5	43/F	craniopharyngioma	amnesia, confusion	gross total removal	temporal lobe infarction	SD
6	59/F	hydrocephalus	amnesia, confusion	ventriculo-cisternal communication	none	MD
7	27/M	hydrocephalus	drowsy state	ventriculo-cisternal communication	none	MD

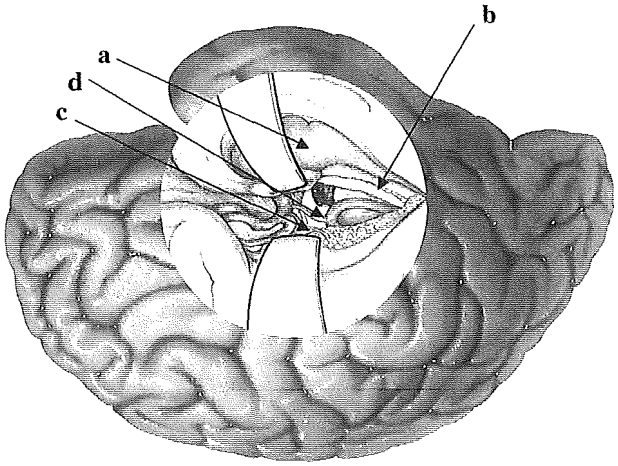

Fig. 1. Schematic drawing of the transsylvian trans-limen insular approach. By cutting the inferior limiting sulcus of the insular cortex, the inferior horn of the lateral ventricle (*a*) is exposed. The inferior part of the choroidal fissure (*b*) is dissected and the inferior border of the limen insula is split to expose the crural (*c*) and anterior part of the ambient cisterns (*d*)

dolicho-ectatic internal carotid artery. The aneurysm was located in the crural cistern and ruptured into the inferior horn of the lateral ventricle. For clipping of the neck, splitting of the limen insula was required (Fig. 2). The other 2 cases had aneurysms in the interpeduncular cistern. Both patients were in grade 4 of the WFNS grading scale when they were admitted. One had a posteriorly directed high positioned basilar bifurcation aneurysm and the other had a recurrent wide neck aneurysm at the origin of the right superior cerebellar artery (Fig. 3). We considered that the supero-lateral access to the aneurysm was adequate for the neck dissection from the perforating arteries and the clipping of the aneurysm. For that purpose, we adopted the transsylvian trans-limen insular approach.

In the case of the ruptured temporal lobe arteriovenous malformation (Case 4), the nidus was located in the anteromedial temporal lobe including the amygdala and hippocampus. The main feeding arteries arose from the middle cerebral and the anterior choroidal arteries. The draining veins emptied into the sphenoparietal sinus and the basal vein via the hippocampal vein. The Sylvian fissure was widely opened and the medial surface of the AVM nidus was exposed (Fig. 4). The nidus inferiorly extended to the inferior limiting sulcus of the insular cortex. By dissecting the nidus from the medial temporal surface and the inferior limiting sulcus, the inferior horn of the lateral ventricle was opened. After the total removal of the AVM, the anterior part of the temporal stem had been split and the crural and ambient cisterns had been well exposed.

In a case of the remnant of the craniopharyngioma (Case 5), the exposures of the ambient, crural and interpeduncular cisterns were required for the careful dissection of the remnant of the tumour from the anterior choroidal artery in the crural cistern, the posterior communicating artery and its perforators in the ambient cistern, and the basilar and posterior cerebral arteries in the interpeduncular cistern. We decided to perform the surgery through the transsylvian trans-limen insular approach.

In 2 cases with isolated inferior horn hydrocephalus (Cases 6 and 7), shunt operations were not planned because of repeated shunt malfunction. We intended to create communications to the Sylvian and ambient cisterns, and the inferior horn of the lateral ventricle through the transsylvian trans-limen insular approach.

Operative results

The postoperative courses of the patient with ruptured aneurysm in the crural cistern (Case 1) and the patient with anteromedial temporal lobe AVM (Case 4) were uneventful. They returned to their full active lives without any neurological and socio-psychological abnormalities.